Lithium Diffusion-Efficient Ionogels as Polymer Solid Electrolyte for Next-Gen Lithium-Ion Batteries

Boluwatife Igbaroola, Yassine Eddahani, Patrick Howlett, Maria Forsyth, Luke O'Dell, Nicolas Dupré, Jean Le Bideau

RESEARCH ARTICLE

Energy & Environmental Materials WILEY

Lithium-Ion Batteries

Lithium Diffusion-Efficient Ionogels as Polymer Solid Electrolyte for Next-Gen Lithium-Ion Batteries

Boluwatife Igbaroola, Yassine Eddahani, Patrick Howlett, Maria Forsyth, Luke O'Dell, Nicolas Dupré, and Jean Le Bideau**

The search for safer next-generation lithium-ion batteries (LIBs) has driven significant research on non-toxic, non-flammable solid electrolytes. However, their electrochemical performance often falls short. This work presents a simple, one-step photopolymerization process for synthesizing biphasic liquid–solid ionogel electrolytes using acrylic acid monomer and $P_{111i4}FSI$ ionic liquid. We investigated the impact of lithium salt concentration and temperature on ion diffusion, particularly lithium-ion (Li^+) mobility, within these ionogels. Pulsed-field gradient nuclear magnetic resonance (PFG-NMR) revealed enhanced Li^+ diffusion in the acrylic acid (AA)-based ionogels compared to their non-confined ionic liquid counterparts. Remarkably, Li^+ diffusion remained favorable in the ionogels regardless of salt concentration. These AA-based ionogels demonstrate very good ionic conductivity (>1 mS cm^{-1} at room temperature) and a wide electrochemical window (up to 5.3 V vs Li^+/Li^0). These findings suggest significant promise for AA-based ionogels as polymer solid electrolytes in future solid-state battery applications.

1. Introduction

Lithium-ion batteries (LIBs) have become essential in the quest toward sustainable energy solutions powering a wide range of electronics, cellphones, and electric vehicles.[1,2] Nonetheless, safety concerns about these batteries have persisted as a significant problem for industry experts in recent years. Liquid electrolytes based on organic solvents, which exhibit low thermal stability and high flammability, are combustible, commonly used in conventional lithium-ion batteries and pose a safety risk.[3,4] Should the battery overheat, it may produce internal pressure or leak out the electrolyte and ignite. In order to significantly mitigate this risk, non-flammable electrolytes are needed.[5,6] The industry is reluctant to give up energy density in order to ensure the safety of batteries, although interest in reformulating the electrolyte into extremely non-flammable states like solid or quasi-liquid states is developing.[7] However, challenges such as low ionic conductivity and interfacial problems prevent solid-state batteries from being widely commercialized.

A major progress in battery technology has been made recently with quasi-solid-state lithium battery developments. A promising approach to enhance the safety of lithium batteries involves incorporating ionic liquids (ILs) into solid electrolytes.[7–10] ILs are molten salts, commonly presented as having a melting point of less than ca. 100 °C that contain both organic cations and inorganic or organic anions.[11] They are preferred electrolytes because of their exceptional qualities, which include non-flammability, thermal stability, high ionic conductivity, and a wide electrochemical potential window.[12–14] Nonetheless, ILs' liquid nature presents a number of difficulties for their application in energy storage devices, including high viscosity leading to expected lower conductivity upon salt addition, packing, portability, and leakage concerns.

Ionogels have become a viable quasi-solid electrolyte solution to address these issues. Ionogels are a class of biphasic liquid–solid materials that are generally made by confining ILs in a solid matrix. They provide improved stability over time and keep all of the favorable characteristics of ILs, with the exception of flowability.[9] These confining networks may be made of silica,[15] polymers,[16] or hybrid[17,18] organic–inorganic networks. The chemical and textural characteristics of the confining network, the volume ratio between the IL and the confining network, and the nature of the IL allow for the tuning of the ionogels' properties.[16] In particular, polymers are excellent confinement candidates for ILs to create ionogel electrolytes, which act as both an electrolyte and a separator. Ionogel electrolytes are also sometime shown to have more thermal stability than liquid electrolytes, which would allow lithium batteries made of ionogels to function across a larger temperature range.[1,19,20] Ionogels also appear to be promising for lithium metal battery applications for their ability to slow down the growth of lithium dendrites. Three basic mechanisms by which ionogels prevent the formation of lithium dendrites have been highlighted by recent theoretical studies: Firstly, the high tortuosity of the mechanically robust host network inhibits dendrite growth; secondly, they can form a dense SEI on the lithium anode; and thirdly, the electroosmotic flow of nanopores effectively regulates lithium-ion transport, thereby reducing the driving force for dendrite formation.[21]

While ionogels have demonstrated interesting results in lithium-ion batteries, little is understood about how the diffusion of lithium ions in

B. Igbaroola, Y. Eddahani, Dr. N. Dupré, Prof. J. Le Bideau
Université de Nantes, CNRS, Institut des Matériaux Jean Rouxel (IMN), F – 44000, Nantes, France
E-mail: nicolas.dupre@cnrs-imn.fr
E-mail: jean.lebideau@cnrs-imn.fr
Prof. P. Howlett, Prof. M. Forsyth, Dr. L. O'Dell
Institute for Frontier Materials (IFM), Deakin University, 221 Burwood Highway, Burwood, Vic 3125, Australia
The ORCID identification number(s) for the author(s) of this article can be found under https://doi.org/10.1002/eem2.12811.

DOI: 10.1002/eem2.12811

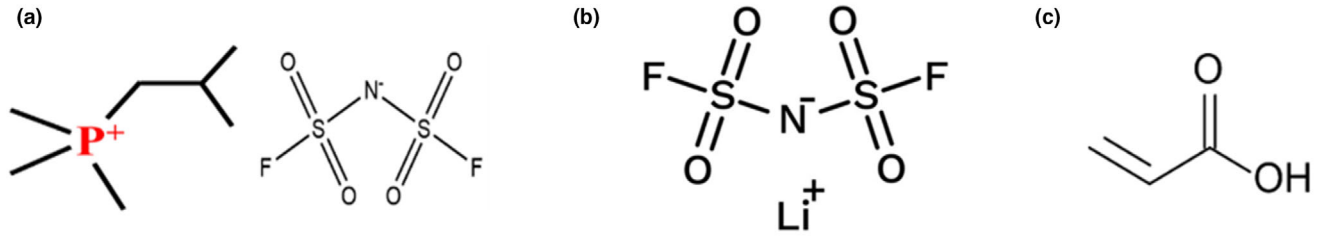

Figure 1. a) P_{111i4}FSI ionic liquid. b) LiFSI salt. c) Acrylic acid monomer.

the confined states differs from that in liquid states (balance between vehicular and Grotthuss-like mechanism, influence of the interface with the host network) and how this affects the devices' performance. Although pyrrolidinium-based ILs have been widely studied for battery applications, recent studies have shown better performance for phosphonium-based ILs especially at higher salt concentrations.[22] Particularly, trimethyl(isobutyl)phosphonium bis(fluorosulfonyl) imide (P_{111i4}FSI) IL has shown a wide electrochemical window, decent ionic conductivity, and reversible cycling different anodes and cathodes.[23,24] The acrylic acid monomer (**Figure 1**c) used herein was selected due to its low molecular weight, good confining properties, and compatibility with lithium-ion batteries, having been used as PAA binder for electrodes.[25] In this study, we synthesized acrylic-acid-based ionogel by confining P_{111i4}FSI IL in acrylic acid polymer by in-situ photopolymerization.

Photopolymerization is a well-known polymerization technique due to its relatively fast process, with a gel point attainable within a short duration of exposure to UV radiation.[26,27] Unlike thermal polymerization, the polymerizable precursor used in photopolymerization does not require the inclusion of rheological stabilizers to avoid creeping prior to heating; it can be cured immediately after deposition. In addition, UV curing uses less energy and is cheaper than thermal polymerization.

We examined by pulsed-field gradient nuclear magnetic resonance (PFG-NMR) the influence of lithium salt concentration and temperature on the diffusion of ions in both the non-confined liquid and the confined (ionogel) electrolytes.

2. Results and Discussion

2.1. Diffusivity of Ions by PFG-NMR

^{1}H NMR can be used to follow the P_{111i4}^{+} cations since their structure includes hydrogen. Likewise, since fluorine atoms are only present in the FSI (and not in the IL cations), FSI anion diffusion can be determined using ^{19}F NMR.[22] ^{7}Li NMR can therefore be used to monitor the self-diffusion of Li ions using the same principle. Generally, a species' molecular weight, size, shape, charge, and solvation environment determine its diffusion coefficient. As a result, these diffusion studies also shed light on the interactions between molecules.

2.1.1. Self-Diffusion Coefficients

Effective ion transport, particularly high Li^{+} mobility, is crucial for achieving optimal device performance. Therefore, we investigated the temperature-dependent diffusivity of Li^{+} ions in both liquid and AA-ionogel electrolytes from 20 to 80 °C, presented in **Figures 2** and **3**. As expected for the non-confined IL, lower concentration (1 M LiFSI) of lithium salt exhibits significantly higher ion diffusivities compared to higher concentration (3 M LiFSI). This trend can be attributed to the higher viscosity associated with the substantial increase in salt concentration within the ionic liquid (IL). Remarkably, the changes in diffusivities between 1 and 3 M LiFSI are less drastic in the confined ionogel electrolyte compared to the non-confined IL (**Figure 4**). For instance, at 80 °C, the ^{7}Li diffusion coefficients in the non-confined ionic liquid (IL) decreased from 1.57×10^{-10} to 6.55×10^{-11} $m^2\,s^{-1}$ upon increasing the salt concentration from 1 to 3 M. In contrast, a minor decrease from 9.28×10^{-11} to 7.16×10^{-11} $m^2\,s^{-1}$ was observed for the confined IL. This result indicates the strong influence of the confinement, probably the influence of interactions at the interface between the liquid and polymer matrix.[9]

For both electrolytes (confined and non-confined), a key observation from the plots (Figures 2 and 3) is the contrasting behavior of Li diffusion coefficients across different salt concentrations. At lower concentrations, the diffusivity of F (D_F) generally appears highest, followed by D_H and D_{Li}. However, upon increasing salt concentration, we observe a significant increase in D_{Li}, potentially exceeding the values for D_H and D_F. This trend in ion diffusivity aligns with previous observation on non-confined ILs by Girard et al.,[11] who reported $D_{Li} > D_H$ at LiFSI concentrations exceeding 2.0 m in P_{111i4}FSI at 22 °C. This faster Li diffusion compared to the P_{111i4}^{+} cation at salt high concentration in the non-confined electrolyte has been attributed to structural rearrangements induced by higher salt content. These rearrangements ultimately lead to a shift in the Li transport mechanism, transitioning from a vehicular-type to an alkali metal (Li^{+}) cation hopping mechanism.[11,22,28] The latter involves ion-exchange and rearrangement of the Li^{+} coordination environment, facilitating Li^{+} hopping across a more interconnected network.

Figure 4 compares the Li^{+} diffusivity (D_{Li}) in non-confined and confined electrolytes across a range of temperatures. At low salt concentrations (1 M LiFSI), D_{Li} values are comparable between the two systems at lower temperatures. Interestingly, at high salt concentrations (3 M LiFSI), D_{Li} remains consistently higher in the ionogel compared to the non-confined electrolyte across all temperatures. Taking a look at the slopes of the plots, there exists a difference between the two systems. At low salt concentration, a lower slope for confined IL signifies a smaller activation energy (E_a) compared to the non-confined IL (see Section 2.1.3), which is consistent with what is observed for high salt concentration: lower E_a and higher D_{Li} whatever the temperature for confined ILs. Higher slopes for the non-confined ILs suggest a temperature-dependent electrochemical performance due to viscosity,

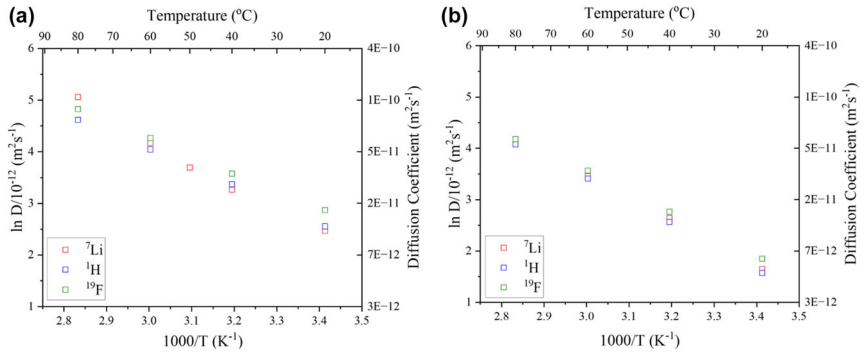

Figure 2. Diffusivity of the ions in non-confined electrolyte at a) 1 M LiFSI and b) 3 M LiFSI concentration measured from 20 to 80 °C.

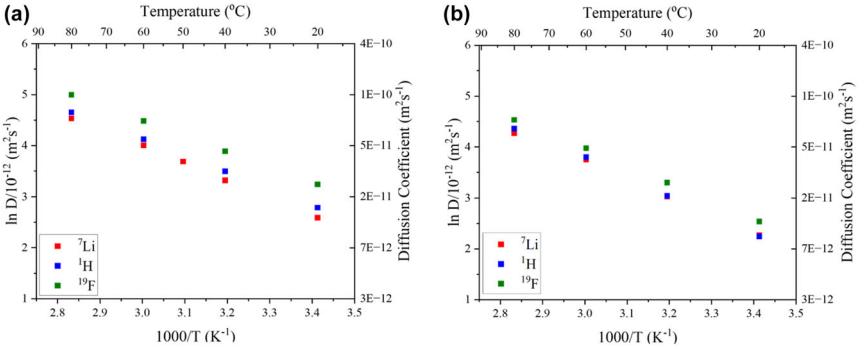

Figure 3. Diffusivity of the ions in AA-based ionogel electrolyte (70% IL confined) at a) 1 M LiFSI and b) 3 M LiFSI concentration measured from 20 to 80 °C.

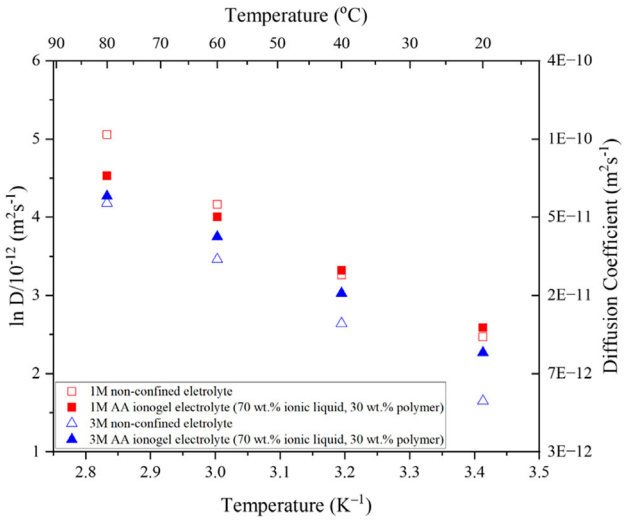

Figure 4. Lithium-ion diffusivities in liquid and confined state at 1 M LiFSI and 3 M LiFSI concentrations measured from 20 to 80 °C.

which could explain why cells assembled with these electrolytes needed to be cycled at 50 °C in previous studies to achieve good electrochemical performance.[11,29]

One would intuitively expect lower D_{Li} values in confined electrolytes due to the potential restriction imposed by the matrix. However, the remarkably high D_{Li} values observed in ionogel electrolytes confirm an enhancement effect arising from the liquid–polymer interface. The two phases in the ionogel are interpenetrated, forming a bicontinuous interface. By confining the ionic liquid electrolyte within the acrylic acid polymer matrix, the ionogel exhibits improved macroscopic transport properties, attributed to higher lithium self-diffusion facilitated by interactions at the liquid–solid interface. Previous work by Demarthe et al. has shown that the enhanced ion diffusion observed in ionogels could be due to new pathways for ion movement created by the solid–liquid interface, along with ionic interactions with the lone pairs of the polyvinylidene fluoride (PVDF) polymer matrix.[16,30] Thus, it is essential to find the optimal balance between the choice of the confining network, the length of the polymer chain, and the amount of ionic liquid confined to achieve superior ionogel performance.[16]

2.1.2. *Apparent Transport Number Comparison*

Building upon the previously discussed results, which suggest a hopping-like/exchange mechanism for Li transport in the high salt concentration phosphonium electrolyte, some uncertainties remain regarding the dominant mechanism governing Li^+ transport in both electrolytes at high salt concentration. While the aforementioned mechanism implies a more efficient Li transport process, further investigation is needed to solidify this hypothesis. Several studies have utilized diffusion coefficients obtained from PFG NMR to estimate the transference number of the lithium ion in electrolytes.[31,32] This work employs a similar approach, but instead of "transference number," the term "apparent transport number" or "diffusivity ratio" is used. This distinction is important because the method employed here includes the transport of charge-neutral ion clusters and does not involve the application of an electric field, a key component of traditional (electrochemical) transference number measurements. This ratio provides valuable insights into ion transport behavior, complementing the existing understanding. The diffusivity of the lithium ion is calculated using the following Equation (1):

$$\mathrm{Dratio}_i = \frac{x_i D_i}{\sum_i x_i D_i}. \quad (1)$$

Dratio_i corresponds to the diffusivity of ion i with respect to all the ions in the electrolyte, x_i the molar fraction of ion_i, and D_i the self-diffusion coefficient of ion i in $m^2\ s^{-1}$.

A substantial increase in diffusivity ratios is observed at 3 M LiFSI compared to 1 M LiFSI, for both confined and non-confined electrolytes. This aligns with previous findings[22,33] that associate higher diffusivity ratios with a hopping/exchange transport mechanism,

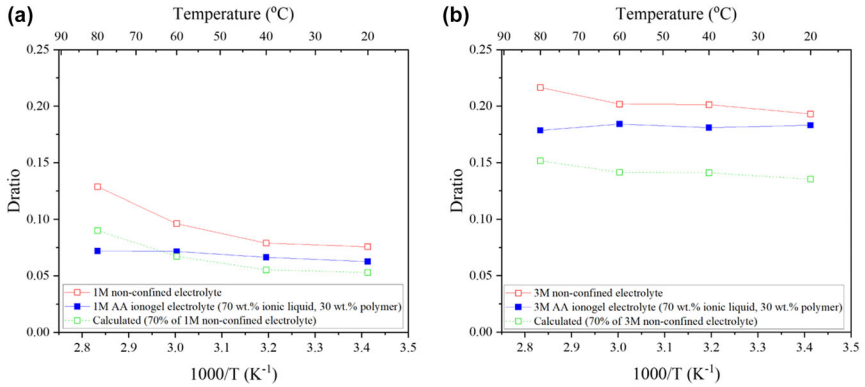

Figure 5. Lithium diffusivity ratios in the non-confined, confined state and expected by calculations at a) 1 M LiFSI and b) 3 M LiFSI concentrations measured from 20 to 80 °C.

typically seen in highly concentrated systems due to the presence of more lithium ions in the electrolyte. As illustrated in **Figure 5**, the non-confined electrolyte exhibits a consistently higher diffusivity ratio compared to the ionogel across all temperatures and concentrations investigated. This finding aligns with the expectation of lower Dratios in ionogels due to their lower ionic liquid (IL) content (70 wt% in this study).

While a high IL content is generally preferred in ionogels to optimize their electrochemical properties due to the dominant role of the confined IL, the polymer component is crucial for ensuring their mechanical integrity. In this study, a 70/30 IL-to-polymer weight ratio was chosen to achieve a desirable balance between mechanical strength and ionic conductivity. While further optimization could potentially increase the IL content, the Dratios obtained for the 70 wt% ionogels remain remarkably high, exceeding predictions calculated based on their composition with respect to the values obtained for the non-confined IL. This observation signifies efficient and relatively rapid lithium transport within the ionogels. It is possible that a further increase in the IL content, toward values like 80% or 90%, could potentially lead to even higher Dratios within the ionogels.

Moreover, the temperature dependence of lithium diffusivity differs significantly between these systems. While the non-confined electrolyte shows a slight increase in diffusivity ratio at temperatures exceeding 50 °C, the ionogels exhibit minimal temperature impact.[34] This further supports the results of Kerr et al.[35] on non-confined ILs, indicating a more efficient Li^+ transport mechanism at moderate temperatures (50 °C) and high salt concentrations in P_{111i4}FSI phosphonium-based electrolytes. This suggests that ionogel electrolytes, with sufficient conductivity and good interfacial properties, could potentially offer comparable electrochemical performance at room temperature to that achieved by liquid electrolytes at higher temperatures.

2.1.3. Activation Energy

The activation energy (E_a) reflects the minimum energy barrier that must be overcome for diffusion to occur. The values of E_a can be determined from the slopes of the ln(*D*) vs 1/*T* plots presented in Figures 2 and 3, covering a temperature range of 20–80 °C. The reported diffusion coefficients of the electrolytes were calculated using Equation (2) and follow the Arrhenius relationship.

$$D = D_o \times e^{\frac{-E_a}{RT}} \quad (2)$$

where D = diffusion coefficient ($m^2\,s^{-1}$), E_a = activation energy ($J\,mol^{-1}$), R = molar gas constant ($8.314\,J\,K^{-1}\,mol^{-1}$), and T = temperature (K).

2.2. ^{7}Li Activation Energy

Lithium-ion batteries rely on the reversible migration of lithium ions (Li^+) between the electrodes during charging and discharging. The electrolyte facilitates the transport of both Li^+ cations and the counter-ions (anions) from the lithium salt. Additionally, separators are crucial for maintaining physical separation between the electrodes while enabling ion movement. Therefore, optimizing Li^+ diffusion within the electrolyte is paramount for efficient battery operation.

The non-confined electrolyte exhibits a decreasing activation energy (E_a) with increasing salt content from 1 to 3 M LiFSI (**Figure 6a**). This is in agreement with the shift in the transport mechanism, possibly toward a more efficient hopping/exchange process at the interface. For the confined IL, the E_a of ^{7}Li diffusion remains relatively unaffected by salt concentration, but in this case, the ^{7}Li Ea is unambiguously lower for the ionogel system compared to that in the non-confined electrolyte, with tendencies as well as values fully consistent with some recent work reported with another polymer host network and a TFSI anion.[30] This shows that Li^+ diffusion in ionogels is inherently easier and more efficient than in the non-confined case, potentially even at lower salt concentrations. Consequently, it appears that ionogels offer the possibility of achieving good electrochemical performance without the need for high salt concentrations, a strategy often associated with low lithium diffusivities at low concentration in liquid electrolytes.

2.3. ^{1}H and ^{19}F Activation Energy

Our investigation also focused on the transport behavior of both the P_{111i4}^+ cation and FSI^- by analyzing their respective ^{1}H and ^{19}F activation energies. Interestingly, the ^{1}H activation energies of the non-confined IL and the ionogel were nearly identical at 0 M LiFSI (Figure 6b). However, upon addition of lithium salt, an increase in ^{1}H activation energy was observed with increasing salt concentration, obvious for the non-confined ILs, and slight, maybe within the experimental uncertainty for the confined ILs. This disparity aligns with the previously observed decrease in ^{7}Li activation energy in the non-confined state at higher LiFSI concentrations suggesting an ease in the diffusion of Li ions and a relatively difficult P_{111i4}^+ diffusion. Collectively, these observations confirm a change in the transport mechanism from vehicular to ion-hopping. However, in the confined case, there seems to be no significant changes in the ^{1}H activation energy across the investigated salt concentration suggesting a lesser impact of a highly concentrated electrolyte.

Analysis of the ^{19}F activation energy (Figure 6c), representing the sole anion in the system, offers insights into FSI^- mobility. Interestingly, ^{19}F activation energies for the non-confined and confined ILs are

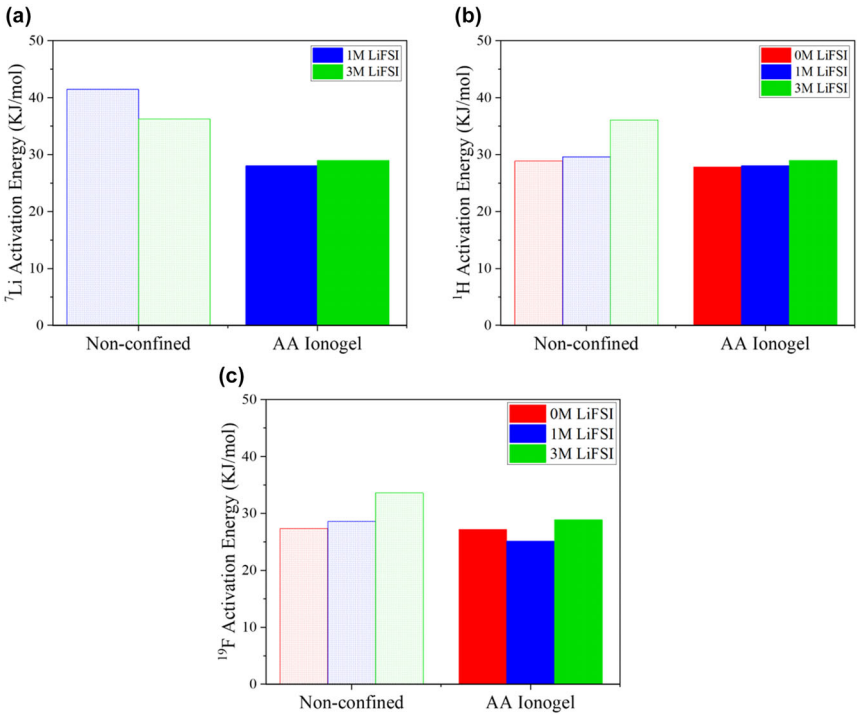

Figure 6. Activation energy (E_a) of the liquid and ionogel electrolytes at 0, 1, and 3 M LiFSI concentration by a) ^{7}Li-NMR, b) ^{1}H-NMR, and c) ^{19}F-NMR.

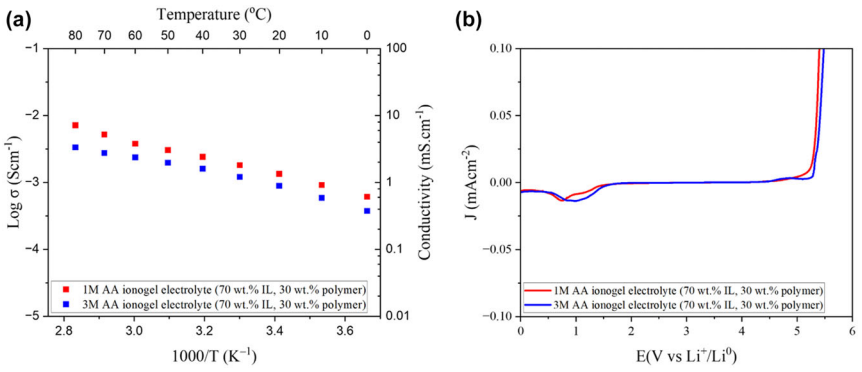

Figure 7. a) Temperature dependency of the ionic conductivity and b) electrochemical stability window of the ionogel electrolytes.

nearly identical at 0 M LiFSI, suggesting comparable initial mobility in the absence of lithium salt. However, upon salt addition, the liquid electrolyte exhibits a significant increase in E_a, reflecting a hindered FSI mobility. While the ionogel also shows a similar trend, the difference in E_a is less significant, suggesting comparatively easier anion movement even at higher salt concentrations, which is consistent with part of the Li^+ cation in interaction with the interface with the polymer and thus less coordinated with the anion.[30] Guyomard-Lack et al.[9] demonstrated that aggregated, structured regions systematically present in bulk ionic liquids (ILs) become disrupted at the interface upon confinement. This "destructuring" of aggregated ion pairs or domains in the ILs enhances lithium diffusion, as evidenced by the lower activation energy observed for the ionogels.

2.4. Ionic Conductivity and Electrochemical Stability

Ionic conductivity is a critical property for battery electrolytes, and the presented results (**Figure 7a**) demonstrate that AA-based ionogels achieve relatively high conductivity despite containing only 70% IL (slightly lower than the values obtained for the non-confined ILs as seen in Figure S1a, Supporting Information). It is worth noting that the reported values account for both the contained ionic liquid and the confining network when calculating the overall conductivity of the ionogel. At both low and high salt concentrations, the ionogel exhibits remarkably high ionic conductivities (1.5 and 1 mS cm^{-1} even at room temperature, respectively) compared to values obtained for solid ceramic electrolytes like LLZO (0.3 mS cm^{-1})[36] or NASICON-type LAGP (0.3 mS cm^{-1})[37] despite being solid-state materials with just 70 wt% of IL confined, suggesting their potential application in lithium-ion batteries.

A broad electrochemical window is crucial for tailoring electrolytes to advanced lithium-ion batteries, particularly those utilizing high-voltage cathodes for enhanced energy density. Figure 7b depicts a typical linear sweep voltammogram (LSV) of the ionogel electrolytes at both low and high salt concentrations, revealing their electrochemical stability up to 5.3 V vs Li^+/Li^0 at 0.1 mV s^{-1} at 50 °C. This stability aligns with the onset of degradation of the liquid electrolyte (Figure S1b, Supporting Information) also reported by Girard et al.,[11] indicating that the incorporated acrylic acid monomer does not introduce additional limitations. The peaks observed between 0 and 1.5 V vs Li^+/Li^0 are associated with the formation of the SEI which was also observed for the non-confined electrolytes.[11] This wide stability window suggests that the ionogel electrolytes could be viable for use with cathodes like $LiFePO_4$ (LFP), $LiNi_{1-x}Mn_xCo_{2-x}O_2$ (NMC), $LiNi_{1-x}Mn_{0.5x}O_2$ (LNMO), and $LiNiO_2$ (LNO), which typically operate within this potential window.

The reversible lithium ions transport through these ionogels and their possible use as solid state electrolyte were validated by cycling them in symmetrical lithium/ionogel/lithium coin cells. Various current densities (0.05, 0.1, 0.2, 0.4, 0.6, 0.8, and 1 mA cm^{-2}) were applied to the ionogels for 1 h during both plating and stripping, with 5 cycles performed at each current density. The evolution of polarization was systematically monitored throughout this process. **Figure 8** illustrates the voltage response of the ionogels at different current densities. Both ionogel concentrations (1 and 3 M) demonstrated the capability to sustain current densities up to 0.4 and 0.6 mA cm^{-2}, respectively, with minimal polarization. However, at higher current

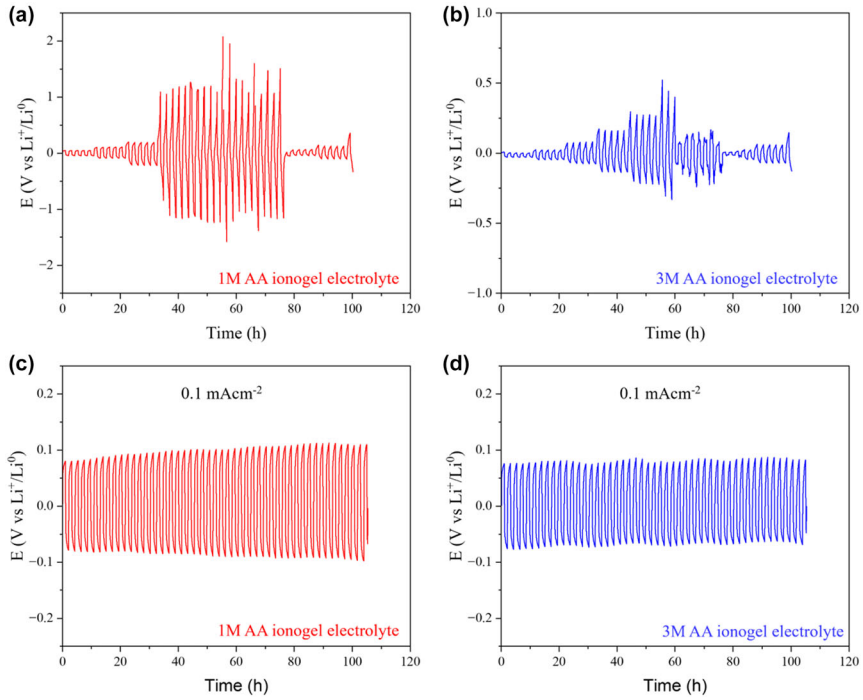

Figure 8. Plating/stripping cycles of lithium symmetric cells with the ionogel electrolytes at variable current densities (a and b) and fixed current density (c and d).

densities, significant polarization was observed, suggesting dendrite formation or electrolyte decomposition. It is worth noting that the 3 M ionogel electrolyte shows a lesser polarization than the 1 M ionogel. This result is in agreement with previous work by Anastro et al.[38] where a high electrolyte concentration facilitates cycling at high current densities despite their lower ionic conductivity. These findings establish the safe operational current limit for the ionogels to be below 0.3 mA cm^{-2} for the 1 M ionogel electrolyte and below 0.6 mA cm^{-2} for the 3 M ionogel electrolyte. Additionally, a constant current density of 0.1 mA cm^{-2} was applied to assess the ionogels' behavior over extended cycling. The ionogels exhibited stable polarization over more than 45 cycles under this constant current density, indicating their stability for long-term cycling applications.

3. Conclusion

This study investigated the transport properties of acrylic-acid-based ionogel electrolytes. Notably, for the confined phase within the ionogels, a significantly better Li^+ diffusivity is obtained compared to the equivalent non-confined liquid. The Li^+ diffusivity in the non-confined state further increases with higher lithium salt concentrations and temperature in contrast to the ionogel with maintained diffusivity. This enhanced Li^+ transport in the confined state compared to the non-confined one is evidenced by lower activation energies for the ionogels suggesting that interactions at the interface between the ionic liquid and the confining polymer matrix enhance Li^+ transport. Additionally, the acrylic-acid-based ionogel electrolytes demonstrate good ionic conductivities (above 1 mS cm^{-1}) and a wide electrochemical window (up to 5.3 V vs Li^+/Li^0), suggesting their potential applicability in energy storage devices. In light of these promising results, our ongoing research efforts are focused on evaluating the cycle life of these ionogel electrolytes within Li-ion battery configurations. The findings from this next phase will be presented in a forthcoming publication dedicated to the electrochemical performance of the AA-based ionogels in both half- and full-cell lithium-ion batteries.

4. Experimental Section

Materials: The acrylic acid monomer used to prepare the confining network and the photo-initiator 2-hydroxy-2-methylpropiophenone were both purchased from Sigma-Aldrich. The ionic liquid, trimethyl(isobutyl)phosphonium bis(fluorosulfonyl) imide: $P_{111i4}FSI$ (Cytec Industries, >99.5%), was purchased from Boron Molecular (Australia), and the lithium salt, bis(trifluoromethanesulfonyl) imide lithium salt (LiFSI), was obtained from Solvionic.

Electrolyte solution and ionogel preparation: The electrolyte solution was prepared by dissolving LiFSI in $P_{111i4}FSI$ with a concentration of 1 M (0.1877 g of Li FSI salt in 1 mL of $P_{111i4}FSI$) and 3 M (0.5631 g of LiFSI salt in 1 mL of $P_{111i4}FSI$) at room temperature in an argon filled glove box. The resulting electrolyte solution is then confined in the acrylic acid polymeric network thanks to the following procedure: The monomer was mixed with the electrolyte solution (IL) in the [30]/70 weight ratio of [monomers]/IL. Then, 1% wt of 2-hydroxy-2-methylpropiophenone was added. 2 h of magnetic stirring, at ambient atmosphere, ensured a good dispersion of the monomers inside the IL. The liquid precursor was transferred into a Teflon mold of diameter 3 mm and depth 15 mm to fit the NMR rotor, and 12 mm diameter, 0.5 mm depth for the electrochemical samples. The precursor was thereafter irradiated using UCUBE-365-025 (250 mW cm^{-2}) from UWave. After 5 min of irradiation, a fully confined network can be obtained. Lastly, each sample was dried at 60 °C under vacuum for 24 h to remove residual water below 50 ppm in the solid electrolyte prior to any NMR or electrochemical experiments, thereby reducing the driving force for dendrite formation.[21]

Diffusivity of the electrolyte ions: Using pulsed-field gradient nuclear magnetic resonance (PFG-NMR), the self-diffusion coefficient of each individual ion in the electrolytes was determined[28] because each ion contains a particular nucleus which can be examined by NMR. The measured self-diffusion coefficients show the contributions from every type of ion and without discriminating between associated and dissociated species. Comparing the overall conductivity measured through PFG-NMR to that measured by electrochemical impedance spectroscopy (EIS) could offer information about the degree of ionicity (free ions) in addition to being helpful for determining the diffusivity of species, specifically while comparing non-confined vs confined ions. The diffusivity of each individual ion in the electrolytes was measured using a pulse-field gradient stimulated echo (PFG-STE) pulse sequence utilizing a Bruker Avance III 300 MHz wide bore spectrometer equipped with a 5 mm Diff50 PFG probe. The measurements were made of the diffusivities of the following nuclei: ^1H, ^{19}F, and ^7Li, which represent the IL cation, FSI anion, and Li ion, respectively. In order to prepare the electrolytes for examination, an argon-filled glovebox was used to fill a 4 mm NMR rotor. The rotor was then placed in a 5 mm NMR tube and sealed with a cap and Teflon tape.[11,39] Using ^1H, ^{19}F, and ^7Li NMR, the diffusivity of the IL cation, FSI anion, and Li^+ was determined, respectively. Measurements were taken for each sample at intervals of 20 °C from 20 to 80 °C. To achieve thermal equilibration, a waiting period of roughly 15 min was allowed to elapse between measurements at various temperatures. In the Topspin software (version 3.5pl7), the T_1/T_2 relaxation analysis module was used to calculate the self-diffusion coefficients, D. Each result is provided with a 5%

margin of error. It is noteworthy that the PFG-NMR approach takes into account a given nucleus in the system, including those on free ions, ion pairs, or larger aggregates, and as such provides average value of the self-diffusion coefficient.[31]

Electrochemical characterizations: Electrochemical impedance spectroscopy (EIS) was used to measure the ionic conductivity of the solid polymer electrolyte between two stainless-steel blocking electrodes at different temperatures (0–80 °C) in incremental steps of 10 °C. The measurement range was 184 kHz to 100 mHz with a sinus amplitude of 150 mV. Using the previously outlined procedure, free samples with an average thickness of 500 µm were generated for this measurement. All potentials are expressed in relation to metallic lithium. By using linear sweep voltammetry (LSV) between lithium and stainless-steel electrodes at scanning speeds of 0.1 mV s^{-1} from OCV to 6.5 and −1 V for the positive and negative electrodes, respectively, the electrochemical stability window at 50 °C was investigated. Lithium/ionogel/lithium symmetrical coin cells were also assembled to evaluate the stripping/plating ability of the synthesized ionogels. All electrochemical experiments were monitored using a VMP Biologic potentiostat/galvanostat operated with EC-Lab software and using Swagelok cells.

Acknowledgements

Boluwatife Igbaroola as a part of the DESTINY PhD program acknowledges funding from the European Union's Horizon 2020 research and innovation program under the Marie Skłodowska-Curie Actions COFUND—Grant Agreement No: 945357. The authors also thank the French-Australian International Research Network IRN-FACES belonging to the French National Center of Scientific Research CNRS for the mobility grant to carry out the PFG-NMR experiments at Deakin University, Australia.

Conflict of Interest

The authors declare no conflict of interest.

Supporting Information

Supporting Information is available from the Wiley Online Library or from the author.

Keywords

diffusion, ionic liquid electrolytes, ionogel, lithium-ion batteries, solid-state batteries

Received: April 26, 2024
Revised: June 21, 2024
Published online: June 25, 2024

[1] L. Carbone, M. Gobet, J. Peng, M. Devany, B. Scrosati, S. Greenbaum, J. Hassoun, *J. Power Sources* **2015**, *299*, 460.
[2] C. M. Costa, E. Lizundia, S. Lanceros-Méndez, *Prog. Energy Combust. Sci.* **2020**, *79*, 100846.
[3] S. Yin, J. Liu, B. Cong, *PRO* **2023**, *11*, 2345.
[4] Q. Wang, P. Ping, X. Zhao, G. Chu, J. Sun, C. Chen, *J. Power Sources* **2012**, *208*, 210.
[5] N. Chawla, N. Bharti, S. Singh, *Batteries* **2019**, *5*, 19.
[6] F. Gebert, M. Longhini, F. Conti, A. J. Naylor, *J. Power Sources* **2023**, *556*, 232412.
[7] N. Chen, H. Zhang, L. Li, R. Chen, S. Guo, *Adv. Energy Mater.* **2018**, *8*, 1702675.
[8] Y. Hu, L. Yu, T. Meng, S. Zhou, X. Sui, X. Hu, *Chem. Asian J.* **2022**, *17*, e202200794.
[9] A. Guyomard-Lack, P. E. Delannoy, N. Dupré, C. V. Cerclier, B. Humbert, J. Le Bideau, *Phys. Chem. Chem. Phys.* **2014**, *16*, 23639.
[10] J. Le Bideau, J. B. Ducros, P. Soudan, D. Guyomard, *Adv. Funct. Mater.* **2011**, *21*, 4073.
[11] G. M. A. Girard, M. Hilder, H. Zhu, D. Nucciarone, K. Whitbread, S. Zavorine, M. Moser, M. Forsyth, D. R. Macfarlane, P. C. Howlett, *Phys. Chem. Chem. Phys.* **2015**, *17*, 8706.
[12] M. Armand, J. M. Tarascon, *Nature* **2008**, *451*, 652.
[13] M. Armand, F. Endres, D. R. MacFarlane, H. Ohno, B. Scrosati, *Nat. Mater.* **2009**, *8*, 621.
[14] D. R. Macfarlane, N. Tachikawa, M. Forsyth, J. M. Pringle, P. C. Howlett, G. D. Elliott, J. H. Davis, M. Watanabe, P. Simon, C. A. Angell, *Energy Environ. Sci.* **2014**, *7*, 232.
[15] P. E. Delannoy, B. Riou, B. Lestriez, D. Guyomard, T. Brousse, J. Le Bideau, *J. Power Sources* **2015**, *274*, 1085.
[16] D. Aidoud, D. Guy-Bouyssou, D. Guy\omard, J. Le Bideau, B. Lestriez, *J. Electrochem. Soc.* **2018**, *165*, A3179.
[17] A. Guyomard-Lack, J. Abusleme, P. Soudan, B. Lestriez, D. Guyomard, J. Le Bideau, *Adv. Energy Mater.* **2014**, *4*, 1301570.
[18] M. Brachet, T. Brousse, J. Le Bideau, *ECS Electrochem. Lett.* **2014**, *3*, A112.
[19] A. Fdz De Anastro, N. Lago, C. Berlanga, M. Galcerán, M. Hilder, M. Forsyth, D. Mecerreyes, *J. Memb. Sci.* **2019**, *582*, 435.
[20] A. Fdz De Anastro, N. Casado, X. Wang, J. Rehmen, D. Evans, D. Mecerreyes, M. Forsyth, C. Pozo-Gonzalo, *Electrochim. Acta* **2018**, *278*, 271.
[21] D. Aidoud, A. Etiemble, D. Guy-Bouyssou, E. Maire, J. Le Bideau, D. Guyomard, B. Lestriez, *J. Power Sources* **2016**, *330*, 92.
[22] K. Araño, D. Mazouzi, R. Kerr, B. Lestriez, J. Le Bideau, P. C. Howlett, N. Dupré, M. Forsyth, D. Guyomard, *J. Electrochem. Soc.* **2020**, *167*, 120520.
[23] D. T. Rogstad, M.-A. Einarsrud, A. M. Svensson, *J. Electrochem. Soc.* **2021**, *168*, 110506.
[24] N. Salem, S. Zavorine, D. Nucciarone, K. Whitbread, M. Moser, Y. Abu-Lebdeh, *J. Electrochem. Soc.* **2017**, *164*, H5202.
[25] P. Parikh, M. Sina, A. Banerjee, X. Wang, M. S. D'Souza, J. M. Doux, E. A. Wu, O. Y. Trieu, Y. Gong, Q. Zhou, K. Snyder, Y. S. Meng, *Chem. Mater.* **2019**, *31*, 2535.
[26] E. Andrzejewska, M. Podgorska-Golubska, I. Stepniak, M. Andrzejewski, *Polymer (Guildf)* **2009**, *50*, 2040.
[27] M. Wang, P. Zhang, M. Shamsi, J. L. Thelen, W. Qian, V. K. Truong, J. Ma, J. Hu, M. D. Dickey, *Nat. Mater.* **2022**, *21*, 359.
[28] M. J. Williamson, J. P. Southall, H. V. S. A. Hubbard, S. F. Johnston, G. R. Davies, I. M. Ward, *Electrochim. Acta* **1998**, *43*, 1415.
[29] L. Porcarelli, J. L. Olmedo-Martínez, P. Sutton, V. Bocharova, A. Fdz De Anastro, M. Galceran, A. P. Sokolov, P. C. Howlett, M. Forsyth, D. Mecerreyes, *Gels* **2022**, *8*, 725.
[30] N. Demarthe, L. A. O'Dell, B. Humbert, R. D. Arrua, D. Evans, T. Brousse, J. Le Bideau, *Adv. Energy Mater.* **2024**, *14*, 2304342.
[31] F. U. Shah, O. I. Gnezdilov, R. Gusain, A. Filippov, *Sci. Rep.* **2017**, *7*, 16340.
[32] T. Frömling, M. Kunze, M. Schönhoff, J. Sundermeyer, B. Roling, *J. Phys. Chem. B* **2008**, *112*, 12985.
[33] M. Forsyth, G. M. A. Girard, A. Basile, M. Hilder, D. R. MacFarlane, F. Chen, P. C. Howlett, *Electrochim. Acta* **2016**, *220*, 609.
[34] S. Bhattacharja, S. W. Smoot, D. H. Whitmore, *Solid State Ionics* **1986**, *18–19*, 306.
[35] R. Kerr, D. Mazouzi, M. Eftekharnia, B. Lestriez, N. Dupré, M. Forsyth, D. Guyomard, P. C. Howlett, *ACS Energy Lett.* **2017**, *2*, 1804.
[36] R. Murugan, V. Thangadurai, W. Weppner, *ChemInform* **2007**, *38*, 7778.
[37] J. Kang, H. Chung, C. Doh, B. Kang, B. Han, *J. Power Sources* **2015**, *293*, 11.
[38] A. Fdz De Anastro, L. Porcarelli, M. Hilder, C. Berlanga, M. Galceran, P. Howlett, M. Forsyth, D. Mecerreyes, *ACS Appl. Energy Mater.* **2019**, *2*, 6960.
[39] C. R. Pope, M. Kar, D. R. MacFarlane, M. Armand, M. Forsyth, L. A. O'Dell, *ChemPhysChem* **2016**, *17*, 3187.